

Electrochemical Reduction of Bicarbonate on Carbon Nanotube-supported Silver Oxide: An Electrochemical Impedance Spectroscopy Study

Soraya Hosseini^{a,*}, Soorathep Kheawhom^a, Salman Masoudi Soltani^b, Mohamed Kheireddine Aroua^c

^aComputational Process Engineering Research Laboratory, Department of Chemical Engineering, Faculty of Engineering, Chulalongkorn University, Bangkok 10330, Thailand

^bDepartment of Mechanical, Aerospace & Civil Engineering, College of Engineering, Design and Physical Sciences, Brunel University London, London UB8 3PH, United Kingdom

^cResearch Centre for Nano-Materials and Energy Technology (RCNMET), School of Science and Technology, Sunway University, Bandar Sunway, 47500, Petaling Jaya, Malaysia

*Corresponding author's Tel: +60176515750

*Corresponding author's e-mail: soraya20h@gmail.com

Abstract

Bicarbonate reduction on a silver-oxide (Ag_2O)-based electrode was studied *via* cyclic voltammetry and electrochemical impedance spectroscopy techniques. The effects of electrode composition, electrolyte concentration and the scan rate (10 - 250 mV/s) were investigated at a temperature of 27 °C. An optimum mass ratio of 70/30 ($\text{Ag}_2\text{O}/\text{CNT}$) led to a maximum current density of 83 mAcm^{-2} at -0.43 V (VS Ag/AgCl). At scan rates between 10 to 250 mV/s, a negative shift with a displacement of around 1.032 V was observed - indicating the presence of irreversible reduction reactions. The observed irreversibility suggested that the reaction mechanism can be described by both diffusion and adsorption phenomena. The standard heterogeneous rate constant (k_o) and the formal redox potential (E_o) were found to be 1.51×10^{-4} cm/s and 1.218 V, respectively. The EIS results confirmed the formation of the inductive loops at reduction potentials - a consequence of the adsorption of the generated species. A reduction in charge transfer resistance and a continual drop in the potential from -0.1 down to -1.4 V was also observed. This was accompanied by H_2 evolution

and bicarbonate production. The calculated pKa value of 10.20 upon the completion of the bicarbonate reduction reactions, confirmed the conversion of bicarbonate to carbonate ions.

Key words: Silver oxide; Bicarbonate; Electrochemical reduction; Impedance spectroscopy

1. Introduction

Carbon dioxide (CO₂) emissions from fossil fuel-fired power plants (*e.g.* coal, natural gas and oil), transportation, industry and residential are the key contributors to greenhouse gas (GHG) emissions [1]. The United States is accounted for around 14.69 % of global CO₂ emissions as the primary greenhouse gas after China - the biggest emitter of carbon dioxide at around (23.4%) [2]. The increased release of GHG, and particularly CO₂, has led to the progressive climate change and global warming and has caused serious environmental damages including polar melting, ocean acidification, melting glaciers, rising sea levels (coastal erosion and flooding of low-lying land and cities), increasing the severity of tropical storms and human health. Various strategies have been suggested and tried in order to mitigate CO₂ emission. These include the improvement of fuel efficiency of cars, utilization of renewable energy resources (solar, wind and wave power), enhancement of energy efficiency in buildings and carbon capture and sequestration (CCS). However, a tangible emission reduction could be only achieved with the help of the development of novel and more energy-efficient processes [3-5].

Recycling CO₂ into readily-transportable hydrocarbon fuels and valuable chemicals *via* photochemical, biochemical and electrochemical reduction methods, has increasingly gained attention as a solution to both the energy and environmental challenges of the world today [6, 7]. Moreover, electrochemical reduction is a promising method, due to its operability under ambient reaction conditions and the ease of process control. In addition, unlike photochemical and biochemical processes, less limitation is associated with the

electrochemical reduction technologies in converting CO₂ into value-added chemicals. Universally, the core research goal has been centred on the improvement of the process efficiency and product yield [8, 9]. The CO₂ reduction process is initiated in large negative potentials and generates C-intermediates that are thermodynamically unstable. Hydrogen evolution, as a competitive reaction, can be promoted in CO₂ electrochemical in an aqueous electrolyte *via* the utilization of a large negative potential. Therefore, development of novel electrocatalysts is vital in order to control and improve product selectivity [10, 11].

Different catalytic metals have been used in the production of various fuels and hydrocarbons *via* electrochemical reduction of CO₂. Several studies have demonstrated that some catalysts such as silver (Ag), gold (Au), copper (Cu) and zinc (Zn) are able to co-produce CO and H₂. However, Ag and Au are more selective towards the production of CO [12]. This product (*i.e.* CO and H₂ - known as syngas) can then be converted into liquid fuels *via* the well-known Fischer-Tropsch process [13]. Some earlier works have studied the effect of an Ag-based cathode to generate CO *via* CO₂ reduction. It has been reported that silver-based catalysts correspond to a higher CO selectivity due to the weak binding energies of CO on the catalyst's surface. Hoshi et al. 1997 studied the electrochemical reduction of CO₂ on pure-metal crystals: Ag (100), Ag (110) and Ag (111). In these studies, a higher current density was observed for Ag (110) as compared to Ag (111) and Ag (100) [14]. Several electrocatalysts including Ag bulk [15], immobilized Ag [16], Ag-nanoparticles [17], roughened Ag surface [18], bimetallic alloy Ag/Au [19], Ag/TiO₂ [20] and Ag/graphene [21] have also been reported for CO₂ reduction, with CO and H₂ as the main products. CO is generally adsorbs weakly on Ag and is hardly detected by vibrational spectroscopy [22]. Electrochemical reduction of CO₂ to CO on polycrystalline silver was greatly improved using a thin Ag₂O upon an anodization treatment [23]. Ag₂O with carbonic materials as electrode has been used in several applications *e.g.* as supercapacitors [24], as photocatalyst for the

degradation of acidic dyes and bacterial inactivation [25], in zinc-silver batteries [26] and in sensors for the detection of vitamin B2, B6 and ascorbic acid [27].

This paper investigates the efficiency of a silver oxide-based electrode, supported on carbon nanotube, in measuring the degree of bicarbonate reduction. The prepared electrode can also be used as a sensor in renal electrolyte (NaHCO_3 , KHCO_3) excretion in humans. This work therefore, entails the development and characterization of a composite $\text{Ag}_2\text{O}/\text{CNT}$ electrode and its application in electrochemical bicarbonate reduction. The composite electrode was developed using different current collectors. A uniform particle size distribution was observed for the prepared solution, containing Ag_2O , carbon nanotube, nafion (5%) and isopropanol. The current collectors (*e.g.* copper sheet, graphite rod and glassy carbon electrode) were painted using the prepared solution. The effects of catalyst loading (30 to 100 mg), electrolyte concentration (0.1 to 1 M) and scan rate (10 - 250 m/s) on the efficiency of the process were investigated and the activity of the $\text{Ag}_2\text{O}/\text{CNT}$ electrode was compared against that of pure Ag_2O electrode. In our experiments, NaHCO_3 was directly used as the CO_2 source. In order to investigate the electrode/electrolyte interface behaviour, electrochemical impedance spectroscopy (EIS) measurements were employed (open circuit potentials) to further evaluate the electrochemical behaviour of the sodium hydrogen carbonate and composite electrodes (200 kHz to 100 Hz).

2. Experimental

2.1. Chemicals & Materials

Sodium hydrogen carbonate (99.9%), H_2SO_4 (97%) and isopropanol (absolute, 99.5%) were all purchased from a local company. Ag_2O (99.9%) and Nafion solution (5 wt% - dispersed in water) were supplied by Sigma-Aldrich. Multiwalled carbon nanotube (20–30 nm in diameter, 0.5–2 μm in length, >95% pure) was purchased from Nanostructured &

Amorphous Materials. Copper sheets were made available by a local market. All chemicals were used without any further purification. Electrolyte solutions were prepared using ultra-pure deionized water.

2.2. Electrode Preparation

All experiments were conducted in an electrochemical cell, equipped with three electrodes at room temperature (27 °C) and under the ambient pressure. Cyclic voltammetry (CV) experiments were carried out using an Autolab Metrohm potentiostat electrochemical workstation. The electrocatalytic activity of the Ag₂O/CNT as the working electrode was measured *via* cyclic voltammetry at a potential scan rate of 50 mV/s (1 to −2 V). An aqueous solution of NaHCO₃ (100 mL) was used as the electrolyte. The current density was determined based on the geometrical area (A) of the electrode. The Ag₂O/CNT ink and the pure Ag₂O were used on different current collectors to act as the working electrode (A = 1.6 cm²). A platinum (Pt) wire and an Ag/AgCl (sat. KCl) were employed as the counter electrode and the reference electrode, respectively. The Ag₂O/CNT ink, containing Ag₂O, carbon nanotube, organic binder Nafion (5%) and isopropanol, was painted on the current collectors. Nafion (5%) was added only as a binder to sustain the mechanical integrity and was not expected to have a major impact on the activity of the electrode under the electrochemical reactions. Initially, Ag₂O (80 mg) was added to isopropanol (5 mL). The mixture was then ultrasonically agitated for 30 min. Nafion (5 μL) and carbon nanotube (20 mg) were next added and the resulting mixture was further sonicated for 30 min to ensure adequate dispersion. For electrochemical testing, the mixture was painted on various current collectors such as copper sheet, graphite rod and glassy-carbon electrode. The painted sheets (area = 1.6 cm²) were then dried under the ambient air to serve as the working electrode. Sodium bicarbonate (NaHCO₃) was used as the CO₂ source. The electrochemical impedance spectroscopy (EIS) measurements were conducted in frequency ranges of 200 kHz – 100 Hz

using the potentiostat (Alpha Analytical SP-300 with EC-Lab V10.12 software). The titration method *via* a Titrino Plus was carried out using H_2SO_4 (0.1 M).

3. Results & Discussion

3.1 Electrochemical Reduction of Bicarbonate

This work describes the development and characterization of a novel $\text{Ag}_2\text{O}/\text{CNT}$ composite electrode and its application in electrochemical reduction of bicarbonate. Three different electrodes were used with copper sheet, graphite rod and glassy carbon as the current collectors. The reduction reaction was carried out in a bicarbonate solution (*i.e.* the CO_2 source). The $\text{Ag}_2\text{O}/\text{CNT}$ electrode (80/20 mass ratio) was used throughout the experiments to identify the optimum current collector based on the product selectivity. The electrochemical behaviour of the $\text{Ag}_2\text{O}/\text{CNT}$ electrode with different metal loadings (30, 50, 70 and 100 mg) was studied through cyclic voltammetry (a standard three-electrode configuration). The effect of the scan rate was studied in order to investigate the reduction mechanism of bicarbonate on the composite electrode (10 to 250 mV/s). The bicarbonate concentration was varied from 0.1 to 1 M NaHCO_3 .

Figure 1 shows the comparison between the three current collectors that were coated using the $\text{Ag}_2\text{O}/\text{CNT}$ ink. Current collectors are the critical segments of electrodes and are responsible for efficient charge transport to the active electrode material. It can be seen that the current density of the copper sheet collector is higher than those of the glassy carbon and the graphite-rod collectors. EIS measurements were conducted to compare electron transfer in copper sheet, glassy carbon and graphite rod in NaKHCO_3 (0.5 M). It is observed that the resistance of the copper sheet and glassy carbon are much lower than that of the graphite rod, indicating a smaller resistance and a facilitated electrical transportation for the course of the electrochemical reactions. The reduction peak (copper sheet) is broader due to the increased

charge transfer (Fig. 1). The CV curves exhibit a single broad cathodic peak reduction around -0.43 V during the reverse scan *i.e.* the reduction of bicarbonate ions and evolution of hydrogen. No extra peak can be observed and only promote bicarbonate reduction and H₂ production with Ag₂O/CNT.

Four sets of Ag₂O/CNT compositions were prepared (Table 1). The electrodes were fabricated by airbrushing a catalytic ink over the current collector (*i.e.* the copper sheet). In all cases, the samples were cycled between -2.0 V and 1.0 V at a scan rate of 50 mV/s. Figure 2 shows the corresponding cyclic voltammetry results, measured for different metal loadings (*i.e.* 30, 50, 70, 100 mg), deposited on the copper sheet (as described previously in the experimental section). The Y-axis corresponds to the ratio between the current and the geometric area of the electrode (A). Cyclic voltammetry experiments revealed that the adsorption of bicarbonate species on the Ag₂O/CNT electrode takes place at similar potentials. A reduction, however, was observed between -2.0 and 1.0 V - depending on catalyst loading. No oxidation peak was observed, suggesting the reduction of bicarbonate ions on the working electrode surface to carbonate ions or other valuable chemicals. The formation of formic acid (formate) was observed at a voltage of -0.41 V. The results show that the anodic contributions are between 0 and 1.0 V, while the cathodic counterparts appear to be between 0 and -2.0 V. On the cathodic end of the CVs (-1.2 V), an increase in the absolute current value can be observed. The sharp reduction is associated with the H₂ evolution. The cyclic voltammogram shows an increase in the reduction peaks associated with the Ag₂O/CNT composite-coated copper sheet when the catalyst loading was increased from 30 mg to 70 mg. It can be easily learnt that the best performance with regards to the reduction reaction is obtained with the copper sheet, coated with Ag₂O/CNT (70/30 mass) (Figure 2). The Ag₂O loading considerably affects the electrocatalytic properties. However, no significant electrocatalytic deviation can be observed with a 30-mg loading of the metal

oxide. It is seen that the CV curves corresponding to the copper sheet coated with Ag₂O/CNT with different catalyst loadings are similar; a reduction peak can be clearly observed for all the Ag₂O/CNT electrodes (Figure 2). In addition, the peaks become broader with an increase in the amount of catalyst used, indicating an enhanced kinetic process with the Ag₂O/CNT composite electrode. No reduction peak was revealed with the bare copper sheet. However, the current density of the copper sheet increased to 15, 48 and 83 mA/cm², when loaded with 30, 50 and 70 mg Ag₂O, respectively. It is worth noting that despite what one would expect from increasing the metal loading (from 30 to 70 mg Ag₂O), the activity did not follow a similar trend. This suggests that the CNT loading did also affect the resulting electrocatalytic activity and the electron conductivity. The results show that the accessible surface area is not proportional to the corresponding metal loading. This is important as the resulting activity is often a function of the actual active surface area. Therefore, for high loadings (*i.e.* pure metal), the Ag₂O particles could be agglomerated and thus, result in a decrease in the total active surface area of the electrode (Figure 3). The appearance of the reduction peak (-0.43 V) follows a similar trend to that of the oxidation peak at positive potentials. The CV curves indicate that the Ag₂O/CNT composite and the pure Ag₂O are both active for the reduction reactions in the NaHCO₃ solution. The pure Ag₂O demonstrates an oxidation peak (0.8 V) which could correspond to the formation of AgO in the NaHCO₃ solution. Wan et al. (2013) studied the effect of electrochemical parameters on the formation and reduction of silver oxides. They reported two oxidation peaks *i.e.* at 0.26 and 0.57 V vs SCE, corresponding to the formation of Ag₂O and AgO in an NaOH solution. The current density of the electrode based on pure Ag₂O reveals a lower performance than that of the Ag₂O/CNT (50/50). This is due to the enhanced dispersion of the catalyst within the carbon nanotube network, leading to an improved electrical conductivity.

With a diluted bicarbonate solution, the CV analysis for the Ag₂O/CNT composite-coated copper sheet shows little hysteresis at a reduction potential close to -0.43 V. Figure 4 illustrates the effect of bicarbonate concentration (0.1 to 1 M NaHCO₃) on the reduction process. It is seen that with a 0.1 M NaHCO₃ solution, a smaller area of the CV curve is obtained. The difference can be linked to the lower conductivity of the 0.1 M NaHCO₃ solutions and diffusion limitations in the pores of the composite electrodes. The larger CV areas are associated with the presence of concentrated bicarbonate ions. This means that the electrochemically-active surface areas consume more bicarbonate ions and thus, increase the current density. In this experiment, even in a low concentration of bicarbonate ions, the reduction peak is observed during the reduction reaction when using the Ag₂O/CNT composite electrode. It can be seen that the reduction peak current shifts towards smaller potentials with an increase in the bicarbonate concentration. With 0.1 M NaHCO₃, bicarbonate ions are present at a lower concentration. The distribution of the bicarbonate ions, close to the electrode surface, is initially uniform; a current started to develop as a consequence of the reduction reactions. The current density is proportional to the surface concentration with an intercept equal to zero. Plotting i_c versus C_o , reveals a linear segment which would not pass through the origin. A large deviation due to a non-zero intercept suggests the presence of adsorbed species. The linear relation between i_c versus C_o , follows equation (1) for an irreversible reduction process [28]:

$$i_c = (2.99 \times 10^5) A \alpha^{0.5} \nu^{0.5} D_0^{0.5} C_o \quad (1)$$

where i_c is the peak current (mA), α is the electron transfer coefficient, D_0 is the diffusion coefficient (cm²/s) and C_o is concentration (mol/cm³), A is the surface area (cm²) and ν is the scan rate (mV/s).

The linear relation between i_c versus C_o follows the equation:

$$i_c = 387.95C - 69.318 \quad (R^2 = 0.984) \quad (2)$$

To further conceptualize the charge transfer, the CV curves for the Ag₂O/CNT composite electrode were obtained at various scan rates (10 to 250 mV/s) in a 0.5 M NaHCO₃ solution (Fig. 5). It is observed that with an increase in the scan rate, the peak current linearly increases. Figure 5 shows the varying baseline (cathodic peaks) as a function of the scan rate (10 to 250 mV/s). However, the anodic peaks are less dependent on the scan rate. The cathodic peaks can be split into three distinct regions: charge transfer regions, diffusion-controlled regions and mixed charge transfer–diffusion controlled regions [29]. The cathodic peak current is proportional to the square root of the scan rate according to equation 1. The plot of i_c vs. $V^{0.5}$ is useful in the characterization of the electrochemical reduction reaction (equation 3). The peak currents increase linearly as a function of the square root of the scan rate for irreversible electron transfers.

$$i_c = -50.166v^{0.5} - 5.437 \quad (R^2 = 0.9665) \quad (3)$$

The logarithm of the cathodic peak current (i_p) versus the logarithm of the scan rate (v) is linear (10 mV/s < scan rate < 250 mV/s):

$$\log i_c = 0.3419 \log v + 3.8547 \quad (R^2 = 0.9544) \quad (4)$$

The slope (*i.e.* 0.3419) is different from the theoretically-expected value of 0.5 for diffusion-controlled processes. These findings indicate that for the studied potentials, the process is not fully diffusion-controlled when using the Ag₂O/CNT electrode. The reduction peak shifts towards the larger negative potentials with an increase in the scan rate from 10 to 250 mV/s. At slower scan rates, a noticeable time interval between the oxidation and reduction processes was observed (two peaks). However, at higher scan rates, a different behaviour was observed during the cathodic process: the two cathodic peaks merged into a single peak due to the adsorption of the reactants. Potential (E_p) for an irreversible process is calculated by (Laviron [30]) :

$$E_p = E_o - \frac{RT}{\alpha F} \left[0.78 + 2.303 \log \left(\frac{(\alpha F D_o)^{0.5}}{K^o (RT)^{0.5}} \right) \right] - \frac{2.303 RT}{\alpha F} \log v^{0.5} \quad (5)$$

where α is the transfer coefficient, k^o is the standard heterogeneous rate constant of the reaction, D_o is diffusion coefficient, ν the scan rate and E_o is the formal redox potential. By plotting potential E_p versus $\log \nu^{0.5}$, the transfer coefficient (α) can be calculated from the slope of the resulted plot:

$$E_p = -2.0681 \log \nu^{0.5} - 2.401 \quad (r^2 = 0.8904) \quad (6)$$

E_p is a function of the scan rate, shifting towards the negative direction for reduction by an amount of 1.032 V from equation $1.15RT/\alpha F$ [28] *i.e.* 20% smaller than the experimentally-obtained data (1.221 V) for scan rates between 10 and 250 mV/s. The two parameters, k^o (1.51×10^{-4} cm/s) and E_o (1.218 V), can be estimated from the intercept of the plot *via* nonlinear regression.

Chronoamperometry techniques were employed to estimate the electrochemically-active surface areas of the Ag₂O/CNT (70/30%) electrode. To measure the electrochemically-active surface areas of the electrode, the chronoamperogram of 0.1 M KH₂PO₄ solution, containing 5 mM of K₄Fe(CN)₆ as the redox probe, was recorded. The electrochemical experiments with the composite electrode were performed in an Autolab Metrohm potentiostat, equipped with NOVA 1.10 software. In the chronoamperometric studies, the current for the electrochemical reaction of ferrocyanide, diffusing to an electrode surface, is calculated as (Cottrell equation [31]):

$$I = \frac{nFAD^{1/2}C_o}{(\pi t)^{1/2}} \quad (7)$$

where I is the current (A), n is number of electrons, A is the active area of electrode (cm²), D and C_o are the diffusion coefficient (6.20×10^{-6} cm²/s) and bulk concentration of K₄Fe(CN)₆ (5×10^{-6} mol/cm³), respectively, F is the Faraday constant (96.487 C/mol); while the remaining parameters have their usual meanings.

For a diffusion-controlled process, the I vs $t^{-1/2}$ plot is linear and from the slope, the value for A can be calculated. In our study, a value of 1.935 cm² was obtained by plotting I vs $t^{-1/2}$ -

which is larger than the geometric surface area (*i.e.* 1.6 cm²). This could be due to the porosity of the electrode surface.

3.2 Electrochemical Impedance Spectroscopy Studies

Electrochemical Impedance Spectroscopy (EIS) studies were done in order to compare the electrical conductivity and charge transfer resistance of the Ag₂O/CNT composite electrode. The Nyquist plots of substrates and the composite electrode - with a sine wave of 10 mV amplitude over a frequency range of 200 kHz to 100 Hz - are shown in [Fig. 6](#), [7](#) and [8](#). Each EIS experiment was carried out at a constant voltage for a broad range of voltages (-2.0 to 0.1 V). Nyquist impedance plots for the substrates *i.e.* the copper sheet, glassy carbon and graphite rod in 0.5 M NaHCO₃ at a potential of 0.0 V were also investigated (not shown). In the 0.5 M NaHCO₃ solution and at high frequencies, a half-circle (*i.e.* and arc) is observed on the Nyquist plot, corresponding to the electron transfer process. However, at low frequencies, a linear segment is formed which corresponds to the diffusion-controlled process. The graphite rod shows a half-circle which has the largest diameter compared to the plots for the other two substrates. The copper sheet corresponds to a plot with the smallest arc diameter. With the copper sheet used as the substrate, regardless of the electrode, the electron transfer process is immediate and the electrochemical response is nearly a straight line.

[Figures 6a](#) and [b](#) show the Nyquist plot for the copper sheet in 0.5 M NaHCO₃ (-1.2 to 1.0 V). The plot demonstrates some specific features: there is a fall in the size of impedance spectrum as the potential increases. The impedance arcs (0.1 to 0.7 V, all located in the first quadrant) decreased varyingly with an increase in the potential; the resistance slightly drops as well. The impedance arcs (0.8 to 1 V) are in the first and fourth quadrants. This suggests that an inductive event has occurred at the end of the oxidation reaction. [Fig.6b](#) depicts the plots for the impedance arcs in the reduction reaction (-0.1 to -1 V). The diameters of the impedance arcs have significantly increased. These arcs are all located in the fourth quadrant

for higher frequencies with the sloping lines visible at lower frequencies. By reducing the potential, the impedance plots are wrapped around the X-axis (anti-clockwise) and the capacitive arcs are flipped to the fourth quadrant (the real component of the impedance is negative). A decrease in the slope of the lines is observed as the potential increases from -0.1 to -1 V, indicating the presence of reaction species as a result of the reduction reaction and the electron-transfer. A voltage of -0.3 V is typically required for H₂ to evolve [10]. The second pathway is a conversion of bicarbonate which occurs at a voltage of -0.43 V. The Nyquist plots in the potential zone from -0.1 to -1 V show the inductive phenomenon at low frequencies. This is an indication of inductance in the system. The inductive features depend on the applied potential and the presence of CO on the electrode surface. CO has a very short lifetime due to the interaction with the free metal electrons [32]. The EIS responses at high frequency (0.8 to 1 V) display an inductive behaviour in the potential range (reduction) during which the electrons are injected into the electrode (Fig. 6a). Another pathway opens up the hydrocarbon formation (directly from the CO generation) that is promoted at -0.8 V with copper [33]. At lower potentials (-1 V), arcs with higher diameters appear. This is linked to the generation of various products from bicarbonate reduction and H₂ evolution with the copper sheet used as the electrode.

Figures 7a and b show the EIS spectra of Ag₂O/CNT (70/30%)-coated copper sheet in a 0.5 M NaHCO₃ solution (-1.2 to 1 V). All the EIS curves comprise a half-circle in the high-frequency region and a linear segment in the low frequency area (Figure 7). The half-circle is explained *via* the charge transfer resistance throughout the bicarbonate ion reaction at the interface of the electrolyte and the composite electrode. The linear section represents the retardance characteristic of the composite electrode and can be linked to the ion-diffusion processes in the electrode. The diffusion/transport of ions within the pores or surface roughness of the composite electrode during the reduction reaction affects the shape of the

line. Figure 7a demonstrates the EIS spectra for the oxidation of the Ag₂O/CNT electrode (0.1 to 1 V). The EIS studies show that the diameters of the arcs on the Nyquist plots slightly decrease with an increase in the potential (0.1 to 1 V). A Randles circuit was used in order to model the EIS data. The circuit parameters were estimated using the Z-Fit software. The randomized/simplex fitting method was used to identify the best fit for the model and the experimentally-measured data (Table 2). Figure 7b shows the fitted circuit comprising resistance, capacitance, constant phase element and the Warburg diffusion resistance. The half-circle is associated with the resistance and capacitance elements in parallel.

Figure 8a shows the reduction-based EIS measurements (-0.1 to -0.9 V) where the diameter of the half-circle decreases with a reduction in the potential. Changing the potential has a direct impact on the charge transfer resistance of the composite electrode. The reduction reactions in the bicarbonate solution could decrease the charge transfer resistance at the Ag₂O/CNT interface. The reduction reaction takes place at a potential of -0.43 V. This is due to the catalytic reaction of HCO₃⁻ and the transfer of the proton-electron pair (H⁺ + e⁻) to the composite electrode. The arcs begin to bend and the negative value of the faradaic impedance points out to an inductive event. Inductive loops have been ascribed to electrochemical asymmetries, which are observed within the studied range of potentials. Some hypotheses have been proposed in the literature to explain this phenomenon, including the heterogeneity of the ions distribution inside the electrode to generate concentration cells between different particles of electrode or the phase change of the active material during the EIS measurement [34]. The charge transfer resistance is further decreased by reducing the potential to -1.4 V.

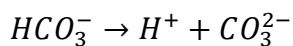
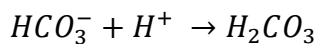
The diameter of the half-circle for Ag₂O/CNT plot at -0.9 V is much smaller than at -0.3 V or -0.1 V potentials (Fig.8a). The semi-circle disappears at potentials above -1 V. The change in the half-circle diameter is the consequence of the variation in the interfacial resistance for the electron transfer from the bicarbonate solution to the electrode surface. The arc gradually

shrinks with an increase in potential (-0.1 V to -1.2 V), indicating the completion of the bicarbonate reduction reactions and H₂ evolution. A decrease in the charge transfer resistance is observed when the potential drops from -0.1 to -1.4 V. [Figure 8b](#) shows a circuit, comprising resistance, capacitance, constant phase element, Warburg diffusion resistance and inductance. The inductance has been included in the circuit due to the inductance phenomenon ([Figure 7b](#)). The charge transfer resistance decreases to around 1 Ω while the capacitance increases, owing to the reduced thickness of the interfacial layer. The cycling performance was investigated in order to test the stability of the electrode/electrolyte over 30 cycles. The results confirm a good stability without any fluctuation.

3.3 Bicarbonate Conversion Studies

Bicarbonate (HCO₃⁻) and carbonate (CO₃²⁻) are defined as the mono and dibasic forms of carbonic acid (H₂CO₃) with Pk₁ and Pk₂ values of 6.35 and 10.33 in water, respectively. Both compounds can be used in pH-jump experiments; from an alkaline pH to a physiological pH. The result of the CV studies show that a cathodic reduction peak appears in bicarbonate solution (-0.43 V) for a pH of around 7.3. The reduction peak is attributed to the aqueous bicarbonate ions which could be reduced on the surface of the electrode. Different kinds of species are typically formed in bicarbonate solutions ([Fig. 9](#)) [35].

In water and depending on the pH, NaHCO₃ is ionised to hydroxide (OH⁻), bicarbonate (HCO₃⁻) and carbonate (CO₃²⁻) ions. The amphoteric bicarbonate ion (HCO₃⁻) can both produce a proton and also consume a proton as in the following reactions:



In our experiments, no significant alkalinity is observed in pH < 4.5. With an increase in the pH (4.5 to 8.3), the concentration of bicarbonate ion increases and reaches a maximum value at a pH of about 8.3. At this point, only the bicarbonate ions are present in the solution. With

a further increase in pH, the bicarbonate ions are converted to the carbonate ions. This conversion is nearly complete at a pH of around 10.2 with almost all of the bicarbonate ions now converted to the carbonate ions. At higher pH values, hydroxide ions - along with the carbonate ions – form [36]. Therefore, the inhibitive effect of the bicarbonate and carbonate ions cannot be separated from each other (unless the pH is different), which would then bring the effect of hydroxide ions into the picture. Several methods have been developed to determine the effect of the ionic concentrations on bicarbonate conversion. In our study, the estimation of the concentrations of the carbonate and bicarbonate ions was done *via* the titration method (end point) in order to determine the concentration of these species before and after the reduction process, according to the equations below [37]:

$$[HCO_3^-] \left(\frac{meq}{L} \right) = \left(\frac{Alk - K_1 \times 10^{pH} + \frac{10^{-pH}}{\gamma}}{1 + 2K_2 \times 10^{pH}} \right) \quad (8)$$

$$[CO_3^{2-}] \left(\frac{meq}{L} \right) = \left(\frac{Alk - K_1 \times 10^{pH} + \frac{10^{-pH}}{\gamma}}{2 + \frac{10^{-pH}}{K_2}} \right) \quad (9)$$

$$[OH^-] \left(\frac{meq}{L} \right) = (K_1 \times 10^{pH}) \quad (10)$$

Where *Alk* is the computed sample alkalinity, *pH* is the initial sample pH, *K₁* is the acid dissociation constant of water, *K₂* is the second acid dissociation constant of H₂CO₃ and γ is the activity coefficient of H⁺ (0.914). The titration was carried out for the bicarbonate solution before and after the reduction reactions *via* the end point method. The reduction reaction was run for 3 hours by using a stainless steel electrode as the anode and the Ag₂O/CNT (70/30 mass) electrode as the cathode (working electrode) in a 0.5 M NaHCO₃ solution. The initial pH is found to be 7.3 (prevalence of HCO₃⁻ ions) with two end points at pH values of 6.81 and 3.97 – indicating the generation of H₂CO₃ and the disappearance of HCO₃⁻. The solution pH increases to 10.32 upon the completion of the reduction reaction. Also, five end points at pH values of 6.28, 3.95, 2.54, 2.1 and 1.82 are observed in the titration. There are five

different regions on the curve for which distinctly-different calculations were done for different ions.

An increase in the solution pH indicates that the bicarbonate ions have been converted to the carbonate ions. Two points (*i.e.* 6.28 and 3.95), have been selected to generate H_2CO_3 and to eliminate the bicarbonate ions. Alk is the alkalinity of the samples and is determined as:

$$Alk = 1000 * V_t * N_a * C_F / V_o \quad (11)$$

Where Alk is the alkalinity of the sample (meq/L), V_t is the volume of titrant needed to reach the equivalence point (ml), N_a is the normality of the acid titrant, C_F is the acid correction factor and V_o is the initial volume of the sample (ml).

The concentrations of the three constituents have been measured before and after reduction. The result of titration analysis shows that the 0.5 M NaHCO_3 solution contains the three ions: OH^- (1.9×10^{-4} meq/L), HCO_3^- (370014 meq/L) and CO_3^{2-} (692 meq/L). After the completion of the reduction reactions, the solution contains: OH^- (0.2089 meq/L), HCO_3^- (212895 meq/L) and CO_3^{2-} (279640 meq/L). The calculated values confirm that the concentration of the carbonate ion has increased significantly while the concentration of the bicarbonate ion has dropped. The pK_a value is calculated from the Henderson-Hasselbalch equation[38]:

$$pK_a = pH + \text{Log} \left(\frac{HA}{A^-} \right) \quad (12)$$

A pK_a value of 10.2 is calculated for the reduction product based on the above equation. This suggests that the bicarbonate ions are converted to the carbonate and hydroxide ions. The reduction product was added to 0.5 M CaCl_2 solution where a white precipitate was immediately formed due to the presence of calcium ions. This means that the CO_3^{2-} ions have been generated in the solution after the reduction reactions. The functional groups in the liquid solutions before and after the reduction reactions as well as on the precipitated solid were determined using FTIR spectroscopy (Fig. 10). The protonated/deprotonated state shows a distinct absorption band which depends on the solution pH. For the

bicarbonate/carbonate solution, at pH values higher than 11 and less than 8, the relative abundance of all the species did not change significantly with pH[39]. The spectrum confirms that the samples have distinct surface functional groups. The peak at 3310 cm^{-1} is assigned to the stretching of the OH group. The FTIR studies have been done both before and after the reduction reactions. The bicarbonate ions show two distinct bands at 1635 cm^{-1} and 1340 cm^{-1} which are assigned to the asymmetric and symmetric stretching vibrations of CO before the reduction reaction, respectively. The carbonate group also shows a broad and intense absorption band in the spectral range of 1630 cm^{-1} and a weak absorption band at 1390 cm^{-1} [40,41]. A small shift is seen in both cases between 1340 and 1390 cm^{-1} . Shifting a band to higher or lower values depends on the bond length. If the bond length decreases the peak wave number shift to the larger values and *vice versa*. Changes in the bond length may occur due to a change in the electronegativity of the neighbouring atom *e.g.* hydrogen bonding. Two bands (871 and 1442 cm^{-1}) are assigned to carbonate (out-of-plane bending) and (asymmetric stretching), which are common for both types of carbonate calcium *e.g.* calcite and vaterite. However, based on our FTIR spectra, the presence of vaterite is more probable [42]. Dunwell et al.(2017) studied the role of bicarbonate in the reduction reaction of CO_2 on gold. They concluded that bicarbonate enhances the rate of CO production on the gold surface through rapid equilibrium between bicarbonate and the dissolved CO_2 [43]. Kortlever et al. (2013) investigated electrochemical reduction of CO_2 and bicarbonate on copper with a reduction peak at -0.6 V (vs. RHE) - assigned to the formation of a CO on the copper surface [44]. Reduction of bicarbonate to formate *via* photocatalyst ZnS crystal structure was studied by Leonard et al. (2015) [45]. In addition, the reduction of bicarbonate *via* AgNP and Ag/MCN was studied by Arrocha-Arcos (2017) where the formation of formate was confirmed [46].

Conclusion

The voltammetric behaviour of an Ag₂O/CNT composite electrode was studied at different scan rates and electrolyte concentrations. The prepared electrodes were studied in order to identify the reactions associated with the oxidation and reduction peaks corresponding to Ag₂O. The reduction peak was observed at -0.43 V without the presence of any oxidation peak (anodic), indicating that an irreversible reaction has taken place on the electrode surface. With an increase in the scan rate, the reduction peak density increased and shifted to negative potentials. At higher scan rates, the two peaks coalesced and only one peak appeared.

The experimental results suggest that the processes are diffusion- and adsorption-controlled. The FTIR analyses revealed an increase in the concentration of the carbonate ion, resulted from the interaction of Ag₂O/CNT electrode with the bicarbonate solution. The FTIR results were also successfully used in the analysis of calcium carbonate.

It is worth noting that the production of silver (as in other metal production processes) is associated with the co-generation of a substantial amount of CO₂ and its subsequent release into the environment. Capturing this CO₂ using the prepared electrode in this study could therefore, theoretically, mitigate part of the baseline CO₂ emissions during the production of silver. However, there are specific considerations, including transportation-related emissions, which must be equally taken into account in order to fully understand the techno-economic aspects of the proposed process in this study. In addition to this, the CAPEX and OPEX of a commercial-scale process using the prepared electrode must be fully learnt in order to be able to draw a fair conclusion on not only the process efficiency, but also on the process sustainability and large-scale feasibility.

Acknowledgment

This research was supported by Rachadapisek Sompote Fund for postdoctoral Fellowship, Chulalongkorn University.

References

- [1] Yong Xiang, Maocheng Yan, Yoon-Seok Choi, David Young, Srdjan Nesic, Time-dependent electrochemical behavior of carbon steel in MEA-based CO₂ capture process, *International Journal of Greenhouse Gas Control* 30 (2014) 125–132
- [2] <http://www.worldatlas.com/articles/biggest-contributors-to-global-warming-in-the-world.html>
- [3] Dimitri Mignard, Rakesh C. Barik , Arun S. Bharadwaj , Colin L. Pritchard, Marina Ragnoli ,Franco Cecconi , Hamish Miller , Lesley J. Yellowlees , Revisiting strontium-doped lanthanum cuprate perovskite for the electrochemical reduction of CO₂ , *Journal of CO2 Utilization* 5 (2014) 53–59
- [4] Xiaowa Nie , Wenjia Luo , Michael J. Janik , Aravind Asthagiri , Reaction mechanisms of CO₂ electrochemical reduction on Cu(111) determined with density functional theory, *Journal of Catalysis* 312 (2014) 108–122
- [5] Takeyuki Sekimoto , Masahiro Deguchi , Satoshi Yotsuhashi , Yuka Yamada , Takekazu Masui , Akito Kuramata , Shigenobu Yamakoshi , Highly selective electrochemical reduction of CO₂ to HCOOH on a gallium oxide cathode , *Electrochemistry Communications* 43 (2014) 95–97
- [6] Jiani Qin, Sibow Wang, He Ren, Yidong Hou, Xinchun Wang, Photocatalytic reduction of CO₂ by graphitic carbon nitride polymers derived from urea and barbituric acid, *Applied Catalysis B: Environmental* 179 (2015) 1–8
- [7] Bao Pan, Shijian Luo, Wenye Su, Xuxu Wang, Photocatalytic CO₂ reduction with H₂O over LaPO₄ nanorods deposited with Pt cocatalyst, *Applied Catalysis B: Environmental* 168–169 (2015) 458–464
- [8] Zhihong Yuan and Mario R. Eden , Rafiqul Gani, Toward the Development and Deployment of Large-Scale Carbon Dioxide Capture and Conversion Processes, *Ind. Eng. Chem. Res.*, 2016, 55 (12), pp 3383–3419
- [9] Bhupendra Kumar, Mark Llorente, Jesse Froehlich, Tram Dang, Aaron Sathrum, Clifford P. Kubiak, Photochemical and Photoelectrochemical Reduction of CO₂, *Annual Review of Physical Chemistry*, 63, 2012, 541–589
- [10] Yin-Jia Zhang, Vijay Sethuraman, Ronald Michalsky, Andrew A. Peterson, Competition between CO₂ Reduction and H₂ Evolution on Transition-Metal Electrocatalysts, *ACS Catalysis* , 2014, 4 (10), pp 3742–3748
- [11] Nianjun Yang, Siegfried R. Waldvogel, and Xin Jiang, Electrochemistry of Carbon Dioxide on Carbon Electrodes, *Applied Material and interfaces*, DOI: 10.1021/acsami.5b09825

- [12] M.R. Gonc, alvesa, A. Gomesa, J. Condec, T.R.C. Fernandes, T. Pardala, C.A.C. Sequeirab, J.B. Brancoc, Electrochemical conversion of CO₂ to C₂ hydrocarbons using different ex situ copper electrodeposits, *Electrochimica Acta* 102 (2013) 388–392
- [13] P. Bumroongsakulsawat, G.H. Kelsall, Tinned graphite felt cathodes for scale-up of electrochemical reduction of aqueous CO₂, *Electrochimica Acta* 159 (2015) 242–251
- [14] Hoshi, N., Kato, M. & Hori, Y. Electrochemical reduction of CO₂ on single crystal electrodes of silver Ag(111), Ag(100) and Ag(110). *J. Electroanal. Chem.* 440, 283–286 (1997).
- [15] Toru Hatsukade, Kendra P. Kuhl, Etosha R. Cave, David N. Abram, Thomas F. Jaramillo, Insights into the electrocatalytic reduction of CO₂ on metallic silver surfaces, *Phys. Chem. Chem. Phys.*, 2014,16, 13814–13819
- [16] Cheonghee Kim, Hyo Sang Jeon, Taedaehyeong Eom, Michael Shincheon Jee, Hyungjun Kim, Cynthia M. Friend, Byoung Koun Min, Yun Jeong Hwang, Achieving Selective and Efficient Electrocatalytic Activity for CO₂ Reduction Using Immobilized Silver Nanoparticles, *J. Am. Chem. Soc.*, 2015, 137 (43), 13844–13850
- [17] Amin Salehi-Khojin, Huei-Ru Molly Jhong, Brian A. Rosen, Wei Zhu, Sichao Ma, Paul J. A. Kenis, Richard I. Masel, Nanoparticle Silver Catalysts That Show Enhanced Activity for Carbon Dioxide Electrolysis, *J. Phys. Chem. C* 2013, 117, 1627–1632
- [18] Junwei Zheng, Tianhong Lu, Therese M. Cotton, George Chumanov, Photoinduced Electrochemical Reduction of Nitrite at an Electrochemically Roughened Silver Surface, *J. Phys. Chem. B* 1999, 103, 6567–6572
- [19] Yuki Hamasaki, Naotoshi Nakashima, Yasuro Niidome, Effects of Anions on Electrochemical Reactions of Silver Shells on Gold Nanorods, *J. Phys. Chem. C*, 2013, 117 (6), 2521–2530.
- [20] Luisa F. Cueto-Gómez, Nora A. Garcia-Gómez, Hugo A. Mosqueda, Eduardo M. Sánchez, Electrochemical study of TiO₂ modified with silver nanoparticles upon CO₂ reduction, *Journal of Applied Electrochemistry*, 44, 2014, 675–682
- [21] Joao Henrique Lopes, Siyu Ye, Jeff T. Gostick, Jake E. Barralet, Geraldine Merle, Electrocatalytic Oxygen Reduction Performance of Silver Nanoparticle Decorated Electrochemically Exfoliated Graphene, *Langmuir* 2015, 31, 9718–9727
- [22] Natalia García Rey, Dana D. Dlott, A Structural Transition in an Ionic Liquid Controls CO₂ Electrochemical Reduction, *J. Phys. Chem. C*, 2015, 119 (36), 20892–20899
- [23] Li Qin Zhou, Chen Ling, Michael Jones, Hongfei Jia, Selective CO₂ reduction on a polycrystalline Ag electrode enhanced by anodization treatment, *Chem. Commun.*, 2015, 51, 17704–17707
- [24] Mojtaba Mirzaeian, Abraham A. Ogwu, Hassan Fathinejad Jirandehi, Saule Aidarova, Zhanar Ospanova, Nathaniel Tsendzughul, Surface characteristics of silver oxide thin film

electrodes for supercapacitor applications, *Colloids and Surfaces A: Physicochem. Eng. Aspects* 519 (2017) 223–230.

[25] Devthade Vidyasagar, Sachin G. Ghugal, Aditi Kulkarni, Pragya Mishra, Ashok G. Shende, Jagannath, Suresh S. Umare, Rajamma Sasikala, Silver/Silver(II) oxide (Ag/AgO) loaded graphitic carbon nitride microspheres: An effective visible light active photocatalyst for degradation of acidic dyes and bacterial inactivation, *Applied Catalysis B: Environmental* 221 (2018) 339–348.

[26] David F. Smith, Curtis Brown, Aging in chemically prepared divalent silver oxide electrodes for silver/zinc reserve batteries Author links open overlay panel, *Journal of Power Sources*, 96(2001) 121-127.

[27] Apinya Puangjan, Suwan Chaiyasith, Wipawee Taweeporngitgul, Jeerunda Keawtep, Application of functionalized multi-walled carbon nanotubes supporting cuprous oxide and silver oxide composite catalyst on copper substrate for simultaneous detection of vitamin B2, vitamin B6 and ascorbic acid, *Materials Science and Engineering C* 76 (2017) 383–397.

[28] Allen J. Bard, Larry R. Faulkner, *Electrochemical methods Fundamentals and Applications*, JOHN WILEY & SONS, INC. New Yorke, SECOND EDITION

[29] Milad Rezaei, Seyed Hadi Tabaian, , Davoud Fatmehsari Haghshenas , A kinetic description of Pd electrodeposition under mixed control of charge transfer and diffusion, *Journal of Electroanalytical Chemistry*, 687,2012, 95-101

[30] E. Laviron, General expression of the linear potential sweep voltammogram in the case of diffusionless electrochemical systems, *Electroanal Chem*, 101 (1979), 19–28

[31] M.A. Ajeel, M.K. Aroua, W.M. A. Wan Daud , P-Benzoquinone Anodic Degradation by Carbon Black Diamond Composite Electrodes, *Electrochimica Acta*, *Electrochimica Acta* 169 (2015) 46–51.

[32] E. Zarate, P. Apell, Calculation of low-energy-electron lifetimes, *PHYSICAL REVIEW B*, 60.1999, 2326-2332

[33] J. Ferreira de Brito, A.A. Silva, A.J. Cavaleiro, M. V. Boldrin Zanoni, Evaluation of the Parameters Affecting the Photoelectrocatalytic Reduction of CO₂ to CH₃OH at Cu/Cu₂O Electrode, *Int. J. Electrochem. Sci.*, 9 (2014) 5961 – 5973.

[34] Yuliya Shilina, Baruch Ziv, Aviv Meir, Anjan Banerjee, Sharon Ruthstein, Shalom Luski, Doron Aurbach, Ion C. Halalay, Combined Electron Paramagnetic Resonance and Atomic Absorption Spectroscopy/Inductively Coupled Plasma Analysis As Diagnostics for Soluble Manganese Species from Mn-Based Positive Electrode Materials in Li-ion Cells, *Anal. Chem.*, 2016, 88 (8), 4440–4447

- [35] Ole Pedersen¹, Timothy D. Colmer, Kaj Sand-Jensen, Underwater photosynthesis of submerged plants – recent advances and methods, *Front. Plant Sci.*, <http://dx.doi.org/10.3389/fpls.2013.00140>
- [36] Narayanaru Sreekanth, Kanala Lakshminarasimha Phani, Selective reduction of CO₂ to formate through bicarbonate reduction on metal electrodes: new insights gained from SG/TC mode of SECM, *Chem. Commun.*, 2014,50, 11143-11146
- [37] Frank M. Dunnivant, *Environmental Laboratory Exercises for Instrumental Analysis and Environmental Chemistry*, 28 JAN 2005, John Wiley & Sons, Inc
- [38] Po, Henry N.; Senozan, N. M. (2001). "Henderson–Hasselbalch Equation: Its History and Limitations". *J. Chem. Educ.* **78** (11): 1499–1503
- [40] Maurizio Baldassarre , Andreas Barth , The carbonate/bicarbonate system as a pH indicator for infrared spectroscopy, *Analyst*, 2014,139, 2167-2176
- [41] R.G. Gast, E.R. Landa, G.W. Meyer, The interaction of water (–FeOOH) and amorphous hydrated ferric oxide surfaces, *Clays Clay Miner.* 22 (1974) 31–39.
- [42] M. Falk, The frequency of the H–O–H bending fundamental in solids and liquids, *Spectrochim Acta, Part A* 40 (1984) 43–48.
- [43] Marco Dunwell, Qi Lu, Jeffrey M. Heyes, Jonathan Rosen, Jingguang G. Chen, Yushan Yan, Feng Jiao , Bingjun Xu, The Central Role of Bicarbonate in the Electrochemical Reduction of Carbon Dioxide on Gold, *J. Am. Chem. Soc.*, 2017, 139 (10), pp 3774–3783
- [44] R. Kortlever, K. H. Tan, Y. Kwon, M. T. M. Koper, Electrochemical carbon dioxide and bicarbonate reduction on copper in weakly alkaline media, *Journal of Solid State Electrochemistry*, 17(2013), 1843–1849.
- [45] Leonard DP, Pan H, Heagy MD., Photocatalyzed Reduction of Bicarbonate to Formate: Effect of ZnS Crystal Structure and Positive Hole Scavenger, *ACS. Appl. Mater. Interfaces.* 7(2015)24543-9.
- [46] A.A. Arrocha-Arcos, R. Cervantes-Alcalá, G.A. Huerta-Miranda, M. Miranda-Hernández, Electrochemical reduction of Bicarbonate to Formate with Silver Nanoparticles and Silver Nanocluster supported on Multiwalled Carbon Nanotubes, *Electrochimica Acta*, DOI: 10.1016/j.electacta.2017.06.147